NEOPLASIA
www.neoplasia.com

Volume 11 Number 3 March 2009 pp. 237–246 237

Monitoring of Tumor Promotion and Progression in a Mouse Model of Inflammation-Induced Colon Cancer with Magnetic Resonance Colonography[1]

Matthew R. Young*, Lilia V. Ileva†, Marcelino Bernardo‡, Lisa A. Riffle†, Yava L. Jones§, Young S. Kim¶, Nancy H. Colburn* and Peter L. Choyke‡

*Laboratory of Cancer Prevention, National Cancer Institute, Frederick, MD, USA; †Small Animal Imaging Program, Laboratory Animal Sciences Program, SAIC-Frederick, Inc, Frederick, MD, USA; ‡Molecular Imaging Program, Center for Cancer Research, National Cancer Institute, Bethesda, MD, USA; §Cancer Inflammation Program, National Cancer Institute, Frederick, MD, USA; ¶Division of Cancer Prevention, National Cancer Institute, Bethesda, MD, USA

Abstract

Early detection of precancerous tissue has significantly improved survival of most cancers including colorectal cancer (CRC). Animal models designed to study the early stages of cancer are valuable for identifying molecular events and response indicators that correlate with the onset of disease. The goal of this work was to investigate magnetic resonance (MR) colonography in a mouse model of CRC on a clinical MR imager. Mice treated with azoxymethane and dextran sulfate sodium were imaged by serial MR colonography (MRC) from initiation to euthanasia. Magnetic resonance colonography was obtained with both T1- and T2-weighted images after administration of a Fluorinert enema to remove residual luminal signal and intravenous contrast to enhance the colon wall. Individual tumor volumes were calculated and validated *ex vivo*. The Fluorinert enema provided a clear differentiation of the lumen of the colon from the mucosal lining. Inflammation was detected 3 days after dextran sulfate sodium exposure and subsided during the next week. Tumors as small as 1.2 mm^3 were detected and as early as 29 days after initiation. Individual tumor growths were followed over time, and tumor volumes were measured by MR imaging correlated with volumes measured *ex vivo*. The use of a Fluorinert enema during MRC in mice is critical for differentiating mural processes from intraluminal debris. Magnetic resonance colonography with Fluorinert enema and intravenous contrast enhancement will be useful in the study of the initial stages of colon cancer and will reduce the number of animals needed for preclinical trials of prevention or intervention.

Neoplasia (2009) 11, 237–246

Introduction

Colorectal cancer (CRC) is the third most common cancer in the United States [1,2]. It has been estimated that in 2008 there will be 148,810 new cases of CRC and 49,960 deaths due to CRC [1,2]. Whereas the 5-year survival rate for patients with early stage disease is 90%, more than 57% of patients with newly diagnosed CRC already have regional or distant metastasis at the time of diagnosis [3]. Prognosis becomes increasingly worse with a more advanced disease with a 5-year survival rate of only 10% for those with distant metastases. Thus, early detection of colon cancer is vital to increase survival in CRC.

Abbreviations: ACF, aberrant crypt foci; AOM, azoxymethane; CNR, contrast-to-noise ratio; CRC, colorectal cancer; CT, computed tomography; DSS, dextran sulfate sodium; MPR, multiplanar reformation; MR, magnetic resonance; MRC, MR colonography; MRI, MR imaging; SI, signal intensity; SNR, signal-to-noise ratio; T1W, T1-weighted; T2W, T2-weighted

Address all correspondence to: Matthew R. Young, B576, NCI-Frederick, Frederick, MD 21702. E-mail: youngm@ncifcrf.gov

[1]This article refers to supplementary material, which is designated by Figure W1 and is available online at www.neoplasia.com.

Received 14 October 2008; Revised 30 November 2008; Accepted 8 December 2008

DOI 10.1593/neo.81326

Currently, there are several tests commonly used to screen for CRC, including the fecal occult blood test, digital rectal examination, sigmoidoscopy, barium enema, colonoscopy, and, most recently, computed tomographic (CT) colonography. The fecal occult blood test is limited in its sensitivity for early disease. The digital rectal examination and sigmoidoscopy examine only a limited anatomic section of the colon. Barium enema is a projection technique that is insensitive for early polyps. Colonoscopy allows visualization of the entire colon and detection of aberrant crypt foci (ACF), polyps, and CRC. A particular advantage of colonoscopy is that biopsy can be performed during the examination. The disadvantages of colonoscopy include an unpleasant bowel preparation, the need for sedation, and the potential perforation of the bowel. Moreover, the accuracy of a colonoscopy depends on the skill of the operator to visualize all surfaces of the colon. More recently, magnetic resonance (MR) and CT colonographies are being explored as complementary or alternatives for optical colonoscopy. Both MR and CT colonographies often include computer-generated "flythroughs" of the colon referred to as "virtual colonoscopy." Both offer a less demanding alternative for the patient and allow complete visualization of the colonic surface after the bowel is distended with an enema or with a gas such as air or carbon dioxide.

Recently, animal models of cancer have been engineered to study cancer prevention and early detection [4]. Whereas many of these models take advantage of genetically engineered mice (GEM), the early stages of cancer, starting at the initiated cell, can also be followed after chemically induced carcinogenesis. Chemically induced mouse models of colon cancers result in a more predictable tumor formation that closely resembles the sequence found in human colon cancer [5]. The inflammation-carcinoma model is based on the administration of azoxymethane (AOM), a genotoxic colonic carcinogen, to initiate tumorigenesis followed by dextran sulfate sodium (DSS), an irritant to the colon that induces colitis and promotes tumorigenesis. After 20 weeks, the colon of mice treated in this manner reveal ACF, dysplastic lesions, adenomas, and adenocarcinomas. These lesions have elevated β-catenin, cyclooxygenase 2, and inducible nitric oxide synthase activity [5]. In this two-stage tumor promotion model, a single cycle of 5 to 7 days of exposure to DSS in the drinking water followed by 16 days of normal water is used to induce inflammation of the colon and promote adenoma and subsequent adenocarcinoma formation. By increasing the number of DSS cycles to three, chronic inflammation, which resembles ulcerative colitis or Crohn disease, occurs [6].

Whereas the AOM/DSS model is suitable for intervention studies and can be useful for characterizing both pharmaceutical as well as dietary responses, currently, the mice must be euthanized and their colons must be examined pathologically. Thus, a large number of mice are needed for time course or dose response studies and the progression of disease must be surmised based on different cohorts of animals. Earlier detection of tumor development in live mice that are serially followed with MR colonography (MRC) would reduce the number of mice needed and the time required to perform prevention studies. Repeated imaging of live mice will allow visualization of the tumors as they develop, thus improving understanding of colonic carcinogenesis as well as providing an early indication of efficacy of treatments and more accurate timing for euthanasia for pathologic analysis.

This study describes a method of studying a mouse model of colon carcinogenesis using MRC. A 3.0-T clinical MR imaging (MRI) scanner was adapted for animal use using a dedicated solenoid receiver coil [7]. T2-weighted (T2W) coronal imaging of the colon in the anesthetized mouse was used for detecting acute inflammation. To distend the colon and remove unwanted luminal signal [8,9], an FC-77 Fluorinert enema was used. Fluorinert is an inert, fully fluorinated, nontoxic liquid, which eliminates any MR signal and allows dark lumen imaging with both T1W and T2W imaging. Intravenous gadolinium chelate permitted the enhancement of the bowel wall, inflammation, and tumors. Tumors were detected as early as 29 days after initiation and as small as 1.2 mm^3. The ability to perform dark lumen, contrast-enhanced MRC on a clinical scanner in live animals suggests the potential to translate these studies to the clinic and its valuable for identifying molecular events and response indicators that correlate with the early stages of tumor development.

Materials and Methods

Animals

All animal studies were conducted according to the guidelines set by the Animal Care and Use Committee, NCI-Frederick. Pathogen-free FVB/N mice were purchased from the NCI-Frederick Animal Production Area at 5 weeks of age and were exposed to a 12:12–hour light/dark cycle. Mice were given an AIN-96G purified diet from Harlan Teklad (Madison, WI) and drinking water *ad libitum*. At 6 weeks of age, mice were injected intraperitoneally with AOM (Sigma, St. Louis, MO) at a dose of 10 mg/kg body weight in 0.1 ml of saline (Figure 1). One week later, mice were started on the first cycle of 0, 1%, or 2% DSS 36,000 to 50,000 (MP Biomedicals LL, Solon, OH) dissolved in normal drinking water (reverse osmosis–purified water). Each DSS cycle consists of 5 days with DSS in the drinking water followed by 16 days of normal drinking water. To ensure 100% tumor incidence, some of the animals were treated with a second DSS cycle.

Reagents

Gadopentetate dimeglumine (Gd-DTPA) Magnevist (Bayer HealthCare Pharmaceuticals, Wayne, NJ) was diluted in phosphate-buffered saline (137 mM NaCl, 10 mM phosphate, 2.7 mM KCl, pH 7.4) to a final concentration 80 mM Gd and 50 μl was injected intravenously

Figure 1. Timeline for AOM/DSS treatment. Day 0: mice were injected with a single dose of AOM. Days 7 to 12: mice were treated with of 0, 1%, or 2% DSS in drinking water. Days 28 to 33: some mice were treated with a second cycle of DSS. Mice were imaged by MRI multiple times throughout the study. MR indicates the imaging time points used to generate Figure 3.

(IV; 0.2 mmol/kg for a 20-g mouse) at a rate of 150 μl/min. FC-77 Fluorinert (3M, Minneapolis, MN) was used undiluted.

Magnetic Resonance Colonography

Animals were fasted except for drinking water for 12 hours before the MRC. Magnetic resonance colonography was performed on an Intera Achieva 3.0-T clinical scanner (Philips Medical Systems, Cleveland, OH) equipped with Philips 1.5.4 software and a dedicated mouse solenoid receiver coil. A physiologic monitoring system (Small Animal Instruments, Inc., Stoney Brook, NY) enabled the maintenance of constant temperature and airflow in the anesthesia chamber, a 38-mm OD × 254-mm length clear plastic tube that provides both hearing protection and access for anesthesia gases. It has ports for anesthesia gas, waste gas, and catheter line for IV injection and tubing for the enema. The mice were anesthetized by inhalation of 3% isoflurane and maintained on a mixture of isoflurane/O_2 (1%/1.25%, v/v) throughout data collection. A 20-G gavage syringe was used to deliver an enema containing 0.6 ml of FC-77 Fluorinert (3M) or water. The enema tubing was connected to a syringe pump and maintained at a continuous rate of 25 μl/min to keep the colon distended during the imaging procedure.

T2- and T1-weighted image sequences were applied in the coronal plane with a field of view (FOV) covering the entire colon. A three-dimensional (3D) T2W turbo spin echo image acquisition (time repetition [TR] = 2000 milliseconds, echo time [TE] = 65 milliseconds, turbo spin echo factor = 28, matrix = 256 × 178, FOV = 50 × 35 mm, number of coronal slices = 94, slice thickness = 0.2 mm, scan time = 17 minutes) was synchronized with the respiratory cycle to minimize motion artifacts. A 3D T1W fast field echo imaging was performed (TR/TE = 15/3.3 milliseconds, flip angle = 25°, matrix = 256 × 178, FOV = 50 × 35 mm, coronal slices = 94, slice thickness = 0.2 mm, scan time = 17 minutes) before and after IV contrast injection. After the first scan, 50 μl of Magnevist followed by 50 μl of phosphate-buffered saline was infused at a rate of 150 μl/min into the tail vein through a catheter using a syringe infusion pump (BS-9000-8; Braintree Scientific, Braintree, MA) followed by T1W postcontrast scans. The isotropic resolution allows multiplanar reformation (MPR) of coronal images after the acquisition.

Data Analysis and Tumor Volume Calculations

Data were collected from more than 66 different mice, which were imaged in 134 MRI sessions, where each session included multiple imaging sequences. The data included 40 control sessions, 40 sessions from mice treated with one cycle of 2% DSS, 41 sessions from mice after the second cycle of 2% DSS, seven sessions from mice after one cycle of 1% DSS, and six sessions after two cycles of 1% DSS. To quantitatively assess of the signal intensities (SIs), regions of interest (ROIs) were placed in the lumen and in adjacent tissue. Image noise was determined from an ROI placed outside the animal and defined as the SD of the SIs. The signal-to-noise ratio (SNR) was determined as SI_{lumen} / noise. The contrast-to-noise ratios (CNRs) was determined as (SI_{lumen} – SI_{muscle}) / noise. Multiple 0.2-mm slices from coronal images that spanned the entire colon were used to generate each ROI, which were manually drawn around tumors in each slice using the National Institutes of Health's ImageJ [10] software, and the volume of each lesion was calculated. The sum of the volumes of contiguous tumor ROIs was tabulated. For comparison, volume measurements of colonic lesions were also estimated *ex vivo*. After euthanasia, colons were removed and opened to expose the lumen. Volumes were measured on tumors with clear boundaries in three dimensions using calipers where vol = $\pi r^2 h$.

Results

Experimental Colitis Detected by MRI

DSS added to the drinking water for 5 to 7 days induces an inflammatory response in mouse colon that resembles colitis in humans [11]. At 2 to 3 days after a 5-day exposure to DSS, the colon was imaged by T2W and T1W MRI sequences in the coronal plane without and with intravenous contrast agent. In the normal colon, the distal 2 cm of the descending colon was usually depicted (Figure 2*A*) and the SI was similar to other organs of the abdominal cavity. The lack of water in the stool results in a dark image in T2W (ST). The rectal colon (R) was depicted as it passes though the pelvic region to the anus.

After 5 days of exposure to 2% DSS in the drinking water, the mice showed signs of acute inflammation, as indicated by weight loss, diarrhea, and spotty bleeding. The increased luminal fluids resulting from the inflammatory response is shown in Figure 2*B*. The inflammatory fluid, which has a more intense signal on T2W images, resulted in distention of the colon. The CNR for lumen of the untreated mouse was approximately 11, whereas 3 days after DSS exposure, the CNR for the treated mouse was 25 (Figure 2, *T2W panels*). The distention of the fluid-filled lumen was also visible on T1W images as a hypodense lumen. The increased luminal fluid was even more apparent on T1W images after IV contrast agent. Interestingly, after injection of contrast media, there was an increase in the intralumenal signal indicating leakage of Gd-DTPA into the lumen due to enhance vascular leakiness. The contrast agent fills the lumen from the ascending and transverse colon distally (Figure 2*B*, *right panel red arrowhead*). Thus, the increased SI of the colonic wall in acute colitis in this mouse model is consistent with an increase in secreted intralumenal fluid and suggests a strong inflammatory response. Acute inflammation was confirmed by hematoxylin and eosin (H&E) staining of tissue harvested just after imaging (Figure 2*D*). The acute inflammation resolved 9 days after exposure to DSS (Figure 2*C*) as indicated by the decrease in the CNR from 25 (Figure 2*B*) to 16 (Figure 2*C*) in this mouse.

Detection of Colonic Tumors by MRC with Fluorinert Enema and Intravenous Gadolinium Chelate

Imaging the nondistended colon by MRI is difficult owing to the collapse of the colonic walls. Contrast-enhanced T1W imaging enhances signal from the colonic wall and improves SNR. However, without bowel distention, T1W imaging was insufficient to discriminate the wall from the luminal contents (Figure 2*A*). Administration of water enemas has been used to distend the colon and create a dark lumen [12]. Initially, enemas containing water or Fluorinert, neither of which produce signal in T1W, were compared. The SNR for Fluorinert enema of 0.9 indicated that very little to no signal was being detected from the Fluorinert. Conversely, the SNR for the water enema was 6.5 indicating a modest amount of signal from the water (Figure W1). Moreover, administration of 0.6 ml of Fluorinert by enema just before MRI expanded the lumen and created a dark lumen on both T1W and T2W images, which was not possible with water (Figure 3*A*). The use of the Fluorinert enema for dark lumen MRC provided clear images of the colon from the rectum through the ascending colon. The dark lumen also aided in the depiction of tumors

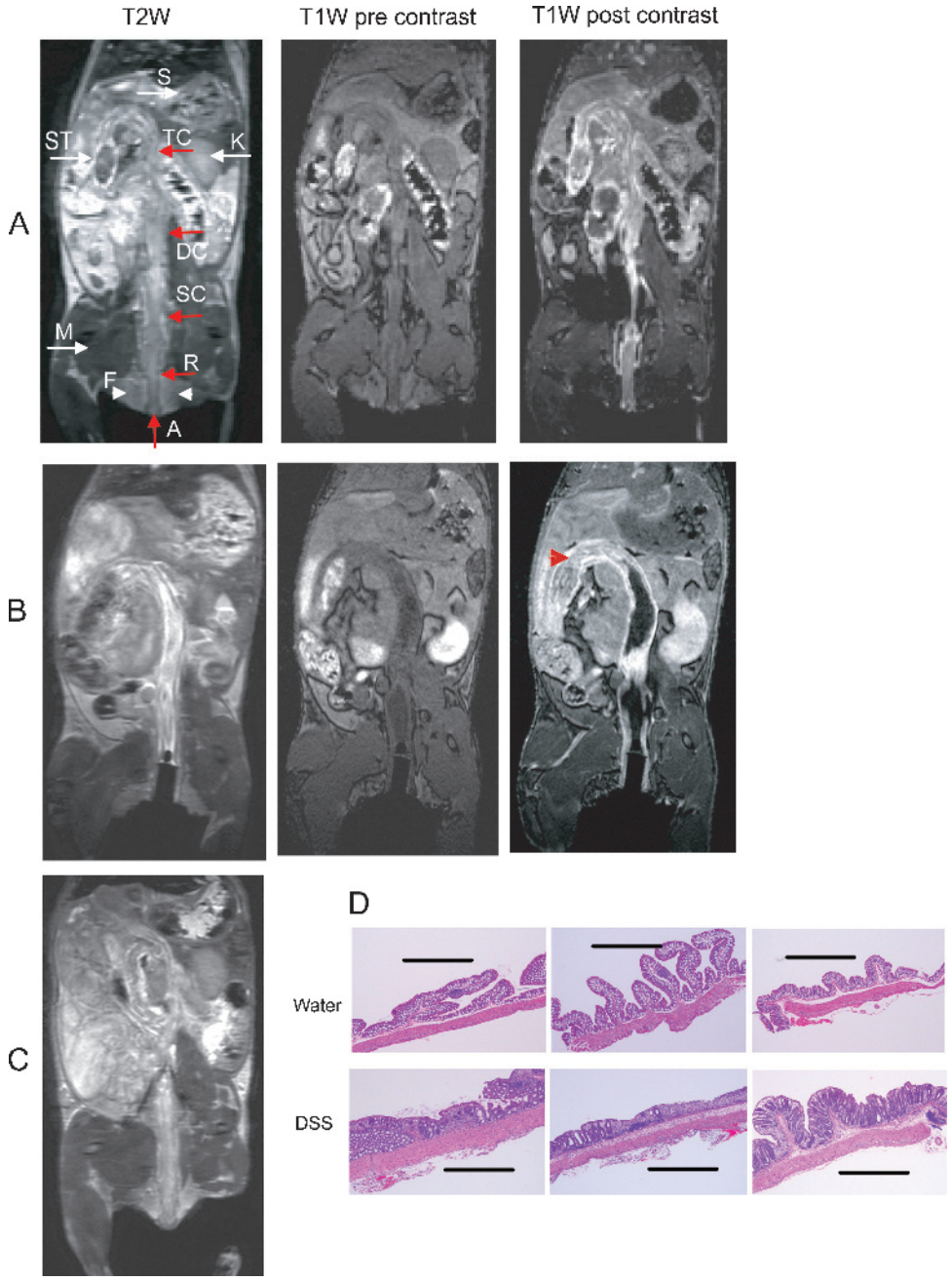

Figure 2. Magnetic resonance imaging shows inflammation 3 days after DSS treatment. T2W and T1W image sequences applied in coronal plane without and with intravenous contrast. Colons were not distended with air or enema. Normal colon (A), inflamed colon 3 days after DSS exposure ended (B), colon recovering from inflammation 9 days after DSS exposure ended (C; T2W only). Red arrows show the anus (A), the rectum (R), sigmoid colon (SC), descending colon (DC), and the transverse colon (TC); white arrowheads show fat (F); white arrows show muscle (M), stool (ST), stomach (S), and kidney (K); and red arrowheads in panel B show luminal contrast agent. (D) Corresponding whole-mount H&E-stained section of colon tissue confirms inflammation 3 days after DSS: normal colon (*top panels*) and inflamed colon 3 days after DSS ended (*bottom panels*). Scale bar, 1 mm.

(Figure 3*B*). The lumen of a mouse 58 days after exposure to AOM/DSS was clearly distended by the Fluorinert enema, and the tumors were distinguishable. As previously reported, dark lumen MRC plus IV contrast media provided the optimal CNR, allowing the clear delineation of tumors in the colon [12].

Three-dimensional MR Images Allow MPR of the Colon

Multiplanar reformation of the coronal images allowed reconstruction in the axial and sagittal planes (Figure 3*C*). The integrity of the mucosal lining was best depicted on the axial plane. In the control animal, the mucosal lining was seen as a uniform layer (Figure 3*C*, *a-a* and *b-b*). During the later stages of tumor progression, the thickness of the mucosa and its enhancement pattern was no longer uniform (Figure 3*C*, *c-c* and *d-d*). The lack of continuous contrast enhancement of the mucosal lining seen in the sagittal MPR indicates nonuniform blood flow to the epithelial tissues during tumorigenesis a potentially important observation about the heterogeneity of angiogenesis during tumor formation.

Magnetic Resonance Imaging Is Useful for Monitoring Progression of Inflammation-Induced Colon Carcinogenesis

In FVB/N mice, which are sensitive to AOM/DSS–induced tumorigenesis, a single cycle of 2% DSS was sufficient to induce inflammation and subsequent tumor promotion after AOM exposure (Figure 4). Mice were treated with a single dose of AOM on day 0, followed by 5 days of DSS starting on day 7. Mice were imaged by MRI at various time points (Figures 1 and 3). All of the images illustrated are from the same mouse except for the untreated mouse. Significant inflammation was seen in the colon 3 days (day 15) after DSS treatment was

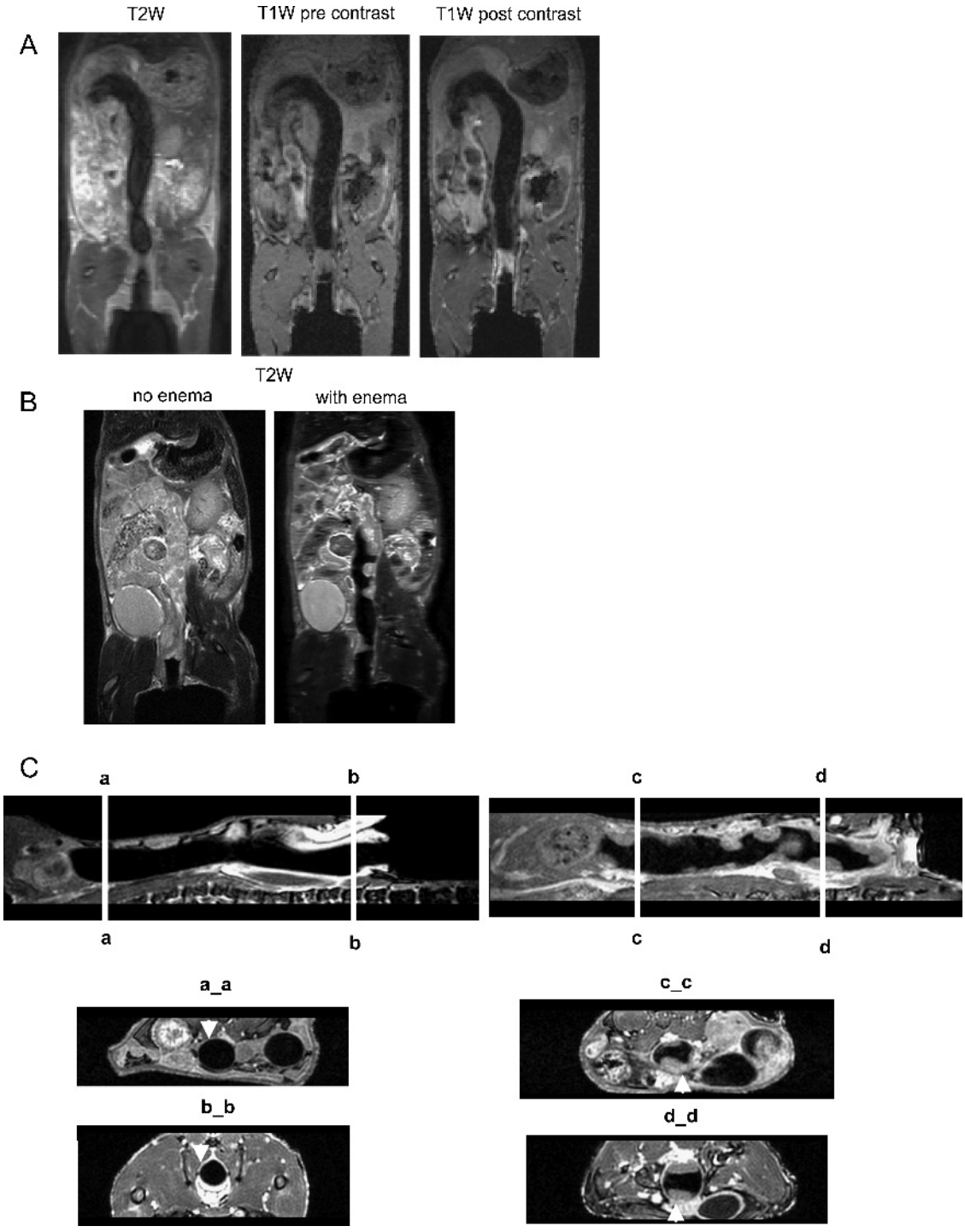

Figure 3. Fluorinert is used to distend and reduce signal from the lumen of the colon. Representative images from MRI sequences applied in coronal plane: (A) T2W, T1W, and T1W with contrast-enhanced coronal images in a healthy colon after Fluorinert enema; (B) T2W coronal images in a tumor-bearing colon: before enema (left panel) and with Fluorinert enema (right panel). (C) Sagittal (top panels) and axial (bottom panels) views after MPR of postcontrast T1 images: normal colon (left panels) and tumor-bearing colon (right panels). Subpanels a-a, b-b, c-c, and d-d indicate the same location in each view. Arrowhead shows healthy mucosal lining (a-a and b-b) and damaged mucosal lining (c-c and d-d).

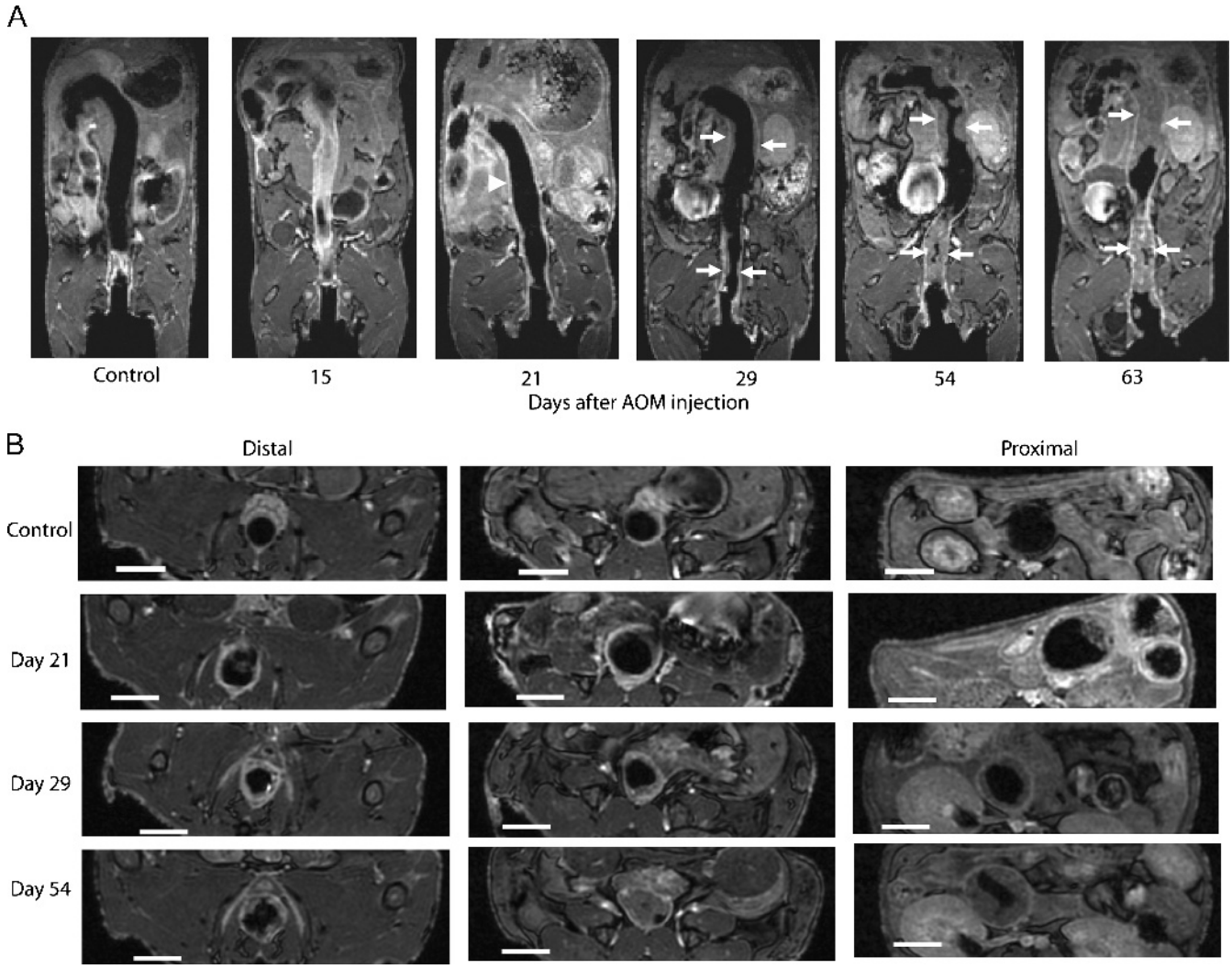

Figure 4. Magnetic resonance colonography is useful for monitoring the progression of inflammation-induced colon carcinogenesis. (A) Mice were imaged with T2W images followed by T1W images before and after contrast. Representative coronal images from T1W MRI sequences after contrast are shown. Except for control, images are from the same mouse imaged on days 15, 21, 29, 54, and 63 after AOM injection. Untreated mouse was injected with AOM but did not receive DSS and was imaged on day 39. Day 15 shows inflammation (contrast bleeding into lumen). Day 20 shows that inflammation has resolved and contrast enhancement of mucosal lining (arrowhead). Day 29 shows beginning of tumor growth (white arrows). Day 50 shows that the same tumors have grown (white arrows) and new tumors have formed. Day 60 shows mouse just before euthanasia. (B) Axial views after multiplanar reformatting of postcontrast T1 images.

completed. In this mouse, intravenous Gd-DTPA was seen leaking into the colon lumen and apparently mixing with the Fluorinert. This mouse also showed weight lost and bloody stools, consistent in acute colitis. The degree of mixing of the contrast agent (hyperintense signal) with the Fluorinert (hypointense signal) increased during the 17 minutes needed for the collection of the images and varied among mice receiving the same treatment (data not shown). In addition, because the mice were more sensitive to the pressure of the enema within the first 3 days after DSS treatment and the possibility of bowel perforation was increased, the use of the enema to monitor acute inflammation was discontinued during the acute phase.

By day 21, 9 days after DSS was completed, the acute inflammation had subsided and the lumen of the colon was again clearly defined by the Fluorinert enema. The mice gained weight, rectal bleeding had stopped, and the mice were able to tolerate the enema. There appeared to be an increase in blood flow to the mucosa as indicated by the increase in contrast enhancement in this area (arrowhead). By day 29, the degree of inflammation decreased and only a small amount of contrast agent was detected in the epithelial lining. At this early time, tumors (seen as asymmetric mounds of tissue) were detected at various locations in the colon. Typically, the tumors measured 2 to 3 mm^3 and extended into the lumen 0.6 to 1.0 mm. By day 54, some of these tumors had grown as large as 25 mm^3 and extended 1.4 to 1.6 mm into the lumen. New tumors were also detected at this time. By day 63, the tumor burden became unsustainable, and the mice were euthanized. Axial MR colonographic views depict the increase in contrast enhancement and the degree of tumor growth into the lumen (Figure 4*B*). Whereas most mice developed tumors in a similar time course, detection of the initial tumor and tumor size varied between mice (see below and data not shown). No visible tumors were detected on multiple images in control mice, treated with AOM but not with DSS, suggesting

that repeated Fluorinert enemas and/or MRI did not promote tumorigenesis (Figure 4*B* and data not shown).

Imaging by MRI Correlates with Ex Vivo *Digital Images*

The standard end point for measuring tumors in this model is 20 weeks (140 days) after exposure to AOM/DSS. At this time, colonic neoplasms adenomas and adenocarcinomas, with dysplastic lesions, mucosal ulcers with focal dysplasia and ACF can be seen histologically [5]. Using MRI, tumors were detected as early as 29 days after AOM (Figure 4). Unfortunately, FVB/N mice are very sensitive to the AOM/DSS treatment, and many mice developed anal prolapse due to their tumors and had to be euthanized before the 20-week end point. For instance, the progression of tumor growth shown for the mouse in Figure 4 was terminated 9 weeks after AOM injection.

After MRC, the colons were removed from the animals and fixed intact. Slices were cut at the approximate distance from the rectum corresponding to the MRI section that demonstrated the lesion (Figure 5, *A–C*). The H&E-stained slides show the presence of the tumors at the estimated locations determined by MRC.

Figure 5, *D–F*, shows a digital photograph of the colon opened to expose the lumen and the H&E staining of tissue taken from this colon. The corresponding tumors seen by MRI are indicated with red arrows. Multiple 0.2-mm MR images confirm the extensive tumor burden seen. Tumor 1 (T1), the most distal tumor, was most consistent with a carcinoma *in situ*. The tumor was endophytic with mild invasion of the submucosa by high-grade dysplastic glandular foci that were distinct from the primary tumor. High-grade dysplasia consisted of mild nuclear pleomorphism, increased mitoses, loss of nuclear polarity, and hyperchromasia. Other lesions in the distal colon had evidence of low-grade dysplasia and polyp formation. Low-grade dysplasia consisted of disorganization of epithelia glands, epithelial hyperplasia with increased mitoses, stratification of nuclei in glands, and loss of goblet cells. Polyps were formed by the dysplastic glands and inflammatory cells. Inflammation was primarily chronic consisting of large numbers of lymphocytes and plasma cells with fewer neutrophils.

A representative volume measurement of multiple tumors from two animals and the corresponding volume determine by caliper measurements are shown in Figure 6*A*. For the eight tumor volumes calculated from MRI *in vivo*, the volume measured *ex vivo* was significantly correlated with each other. Because of the irregular shape and overlapping nature of many of the tumors, an accurate measurement by MR or by caliper for all the tumors was not possible. Figure 6*B* also shows a time course of tumor growth for a single animal. Tumor volumes were determined in the same animal at day 35 and again at day 58. In this mouse, tumor no. 2 measure 1.2 mm^3 on day 35. By day 58, tumor no. 2 had more than doubled in size. It is clear from the MR image that the tumors grow at different rates.

Discussion

The present study describes a method for imaging the early stages of CRC in a mouse inflammation-carcinoma model using a 3.0-T clinical MRI scanner equipped with a dedicated mouse solenoid receiver coil. The use of the Fluorinert enema allows dark lumen imaging by T1W imaging with and without intravenous contrast as well as by T2W imaging. Using T2W MRI in combination with a contrast-enhanced T1W dark lumen MRI, the early stages of tumorigenesis, starting with inflammation, through the advanced tumor growth was followed over time in the same mouse. In the early stages, T2W MRI was used to detect acute inflammation 2 to 3 days after DSS exposure. During this period, the bowel wall was relatively stiff because of the inflammation and was already distended with secretions so that the Fluorinert enema was not necessary. By 7 to 9 days, the inflammation had subsided and the Fluorinert enema became necessary to render the lumen totally dark while sufficiently distended to allow direct depiction of the mucosal wall. Intravenous injection of a gadolinium contrast agent and T1W imaging highlighted the changes in the epithelial lining due to chronic inflammation, hyperplasia, and destruction of the mucosal layer. Tumors as small as 1.2 mm^3 and as early as 29 days were detected after initiation. Individual tumor growth was followed during the course of the study, and volume measurements from MRC *in vivo* correlated with caliper measurements of the tumors *ex vivo*.

Early detection remains the best method of reducing mortality from CRC. The use of animal models allows the design of new and safer methods to screen for early signs of colon cancer. In addition, these models will expand the understanding of the molecular events leading to tumor formation and could help identify new response indicators that correlate with the early stages of tumorigenesis. Finally, these animal models allow preclinical testing of new strategies for prevention and intervention.

The ability of MRI to detect the early stages of colon cancer in mice provides a safe, less-invasive method to monitor the effects of new therapeutics, to determine the optimal time for collection of samples for molecular analysis, and to correlate response indicators to a real-time response in the animal. Magnetic resonance imaging is more appropriate in an animal model than CT because the high radiation doses required for serial mouse imaging during microCT could lead to unwanted perturbations such as increased DNA damage and tumor initiation in these models. Moreover, the use of MRI in animal studies could readily be translated to the clinic. The 3.0-T MRI scanner used in this study is a clinical scanner that was adapted for mouse studies.

Magnetic resonance colonography for detecting and staging colon cancer is being explored in the clinic as an alternative to optical colonoscopy and CT colonography, which are commonly performed in humans [8,13–15]. For either MR or CT colonography, the colon needs to be distended to allow reliable imaging of the colon wall for the assessment of the bowel wall thickness, inflammation, and reliable depiction of tumors. Presently, water-based enemas, air, or carbon dioxide are used to distend the bowels [8,12,16–18]. Recent studies comparing water-based dark lumen MRC with colonoscopy found that the dark lumen MRC was highly accurate in the detection of colorectal masses. In these studies, colonic lesions exceeding 5 mm in size were accurately detected with specificity greater than 95%. In addition, alterations of the colonic wall associated with diverticulitis and inflammatory bowel disease were also detected [12,16]. Lumen distention with CO_2, which may offer less distortion and dephasing artifacts, was used to detect colonic lesions with dark lumen MRC [18]. In addition to distending the colon, a high contrast between the mucosal lining and the lumen is critical for an accurate measurement of tumors. Water enemas are also used for bright lumen MRI where T2W images produce a dark-appearing mucosal wall in a bright lumen background. A gadolinium-based enema combined with T1W images will also produce the bright lumen background. Whereas a gadolinium enema bright lumen MRC allowed a high sensitivity rate, this method has difficulty differentiating between the mucosal lining, residual fecal material, and air bubbles from colonic masses [16]. In the present study, a bright or signal-intense wall with a dark lumen

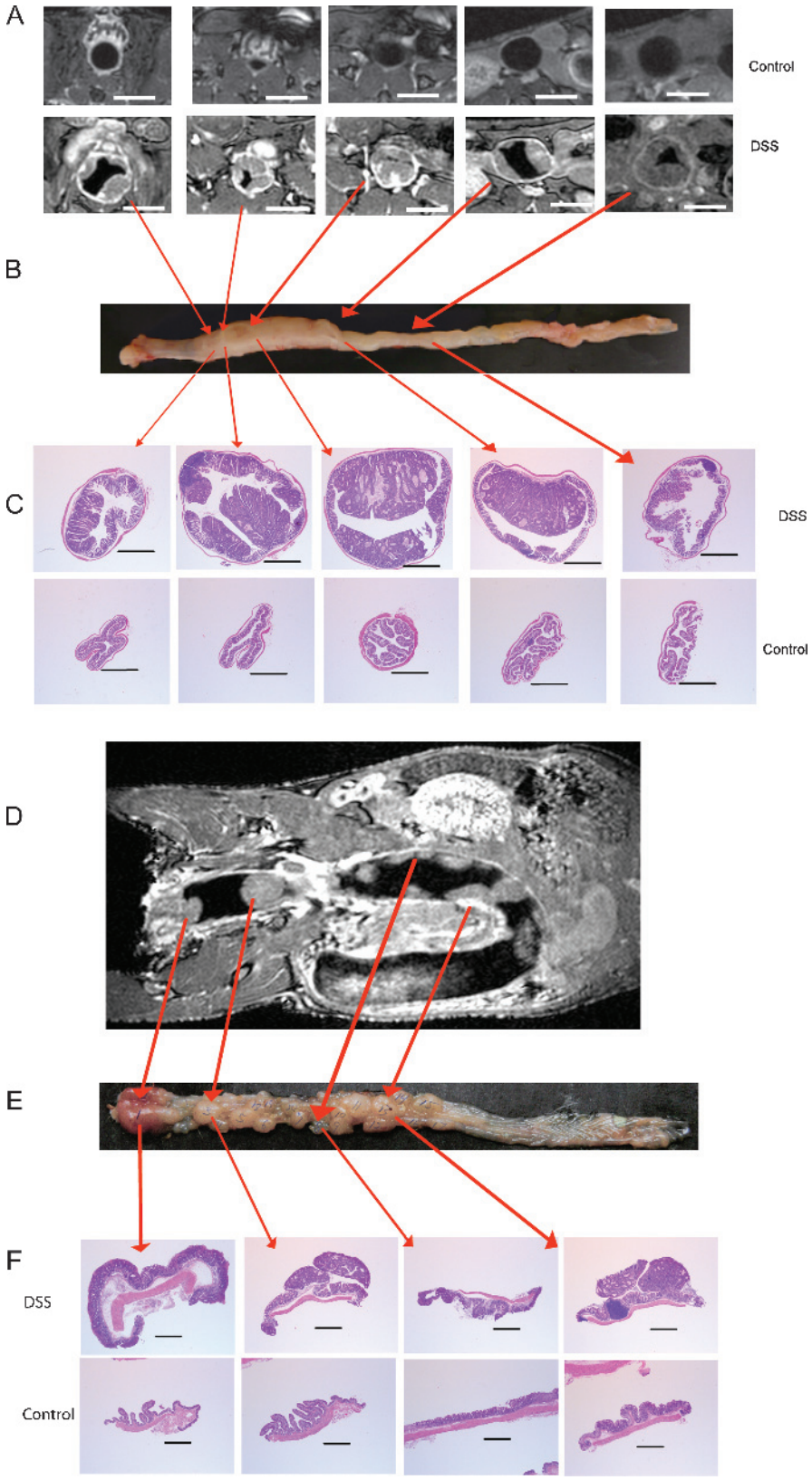

Figure 5. Comparison of MRC with histopathology. Optical photography of the colon *ex vivo* shows multiple tumors. (A–C) Axial MPR and corresponding *ex vivo* images: axial view from MPR (A), optical photography of the same colon shortly after MRI (B), and H&E-stained tissues (C). Locations of tumors were estimated from MRI with ImageJ software. Tissue slices were taken at the corresponding distance from the rectum in the extracted colon. Red arrows indicate estimated location for acquisition of images. Hematoxylin and eosin from untreated control animals are from distal (left) and proximal (right) colon. (D–F) Tumors depicted in coronal view correspond to tumors seen in excised colon with lumen exposed: coronal MRI (D), photograph of the exposed lumen (E), and H&E-stained tissue (F). Tissue slices were taken at the corresponding distance from the rectum in the extracted colon (red arrows). Scale bar in H&E, 2 mm.

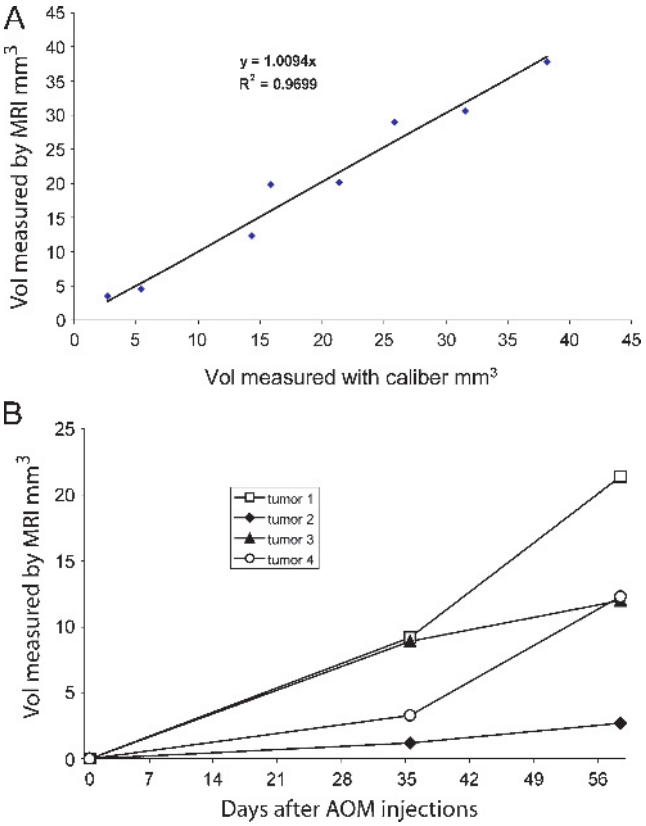

Figure 6. Tumor volumes measured from MRI correlate with volumes measured by caliper. (A) Tumor volume determined from MRI matches closely to the tumor volume measured after necropsy. The volumes of eight tumors from two animals were compared. (B) Individual tumor growth rates were followed over time. Four individual tumor volumes from the same mouse were calculated at days 35 and 58 after AOM. Volumes were calculated from multiple imaging sections using ImageJ and compared with digital measurements from optical images of H&E stains or with *ex vivo* caliper measurements, where vol = $\pi r^2 h$.

background was obtained with both T1W and T2W imaging after distention with Fluorinert, which, unlike water enemas, produced no signal to noise background. Additional contrast was provided by intravenously injected gadolinium chelates, which enhance the colon wall and tumors.

Previous studies demonstrated the value of MRC in the ApcMIN mouse model using a 7-T MRI with a Bruker DRX300 console to image tumors in the colon. A Gd-DTPA–filled silicone tube was used to aid in the identification of the tumors. Whereas tumors as small at 1.5 mm^3 were detected, repeated imaging to follow progression was not reported [19]. In the present study, a Fluorinert enema was used to distend the mouse colon without trauma to the intestinal mucosa. Fluorinert is ideal for dark lumen MRI because it is dark on both T1W and T2W images. Perfluorochemical such as Fluorinert have a high safety profile; they have been safely used for partial liquid ventilation of critically ill premature infants with severe respiratory distress syndrome, and clinical trials to assess the use of perfluorochemical for liquid ventilation have been reported [20,21]. The repeated use of the Fluorinert enema in mice resulted in no detectable toxicity or injury to the bowel. Mice, which were treated with AOM alone and therefore not expected to produce tumors, did not produce tumors even after receiving one or more Fluorinert enemas, suggesting that no additional inflammation was induced by Fluorinert. Although some of the mice with acute inflammation up to 3 days after DSS exposure did not tolerate the enema, most likely due to the pressure of the enema on the compromised mucosal wall, repeated use of the Fluorinert enema at all other times resulted in no detectable toxicity or injury to the bowel. Whereas it is not known whether Fluorinert can cross the epithelial barrier of the colon, there were no visible indications that the enema was creating an inflammatory response in the epithelial tissue.

To efficiently translate information obtained from mouse models of human cancer, it is crucial to incorporate technologies that can rapidly monitor disease progression without requiring the sacrifice of animals at each step. By using minimally invasive methods for detecting and monitoring tumor growth that could be used in the clinic, information derived from the mouse model can more rapidly be translated to the clinic. Magnetic resonance colonography provides a safe and reproducible method for early depiction of premalignant lesions in the mouse colon. The information and efficiencies gained by studying mouse models of colon carcinogenesis with noninvasive imaging techniques such as MRC could accelerate the development of interventions that interrupt the sequence of cancer development in the colon. These interventions might find their way earlier into clinical trials, using imaging techniques similar to those described here.

References

[1] Jemal A, Siegel R, Ward E, Hao Y, Xu J, Murray T, and Thun MJ (2008). Cancer statistics, 2008. *CA Cancer J Clin* **58**, 71–96.

[2] Meissner HI, Breen N, Klabunde CN, and Vernon SW (2006). Patterns of colorectal cancer screening uptake among men and women in the United States. *Cancer Epidemiol Biomarkers Prev* **15**, 389–394.

[3] Ries LA, Wingo PA, Miller DS, Howe HL, Weir HK, Rosenberg HM, Vernon SW, Cronin K, and Edwards BK (2000). The annual report to the nation on the status of cancer, 1973-1997, with a special section on colorectal cancer. *Cancer* **88**, 2398–2424.

[4] Abate C, Brown PH, Colburn N, Gerner EW, Green JE, Lipkin M, Nelson WG, and Threadgill D (2008). The untapped potential of genetically engineered mouse models in chemoprevention research: opportunities and challenges. *Cancer Prev Res* **1**, 161–166.

[5] Tanaka T, Kohno H, Suzuki R, Yamada Y, Sugie S, and Mori H (2003). A novel inflammation-related mouse colon carcinogenesis model induced by azoxymethane and dextran sodium sulfate. *Cancer Sci* **94**, 965–973.

[6] Neufert C, Becker C, and Neurath MF (2007). An inducible mouse model of colon carcinogenesis for the analysis of sporadic and inflammation-driven tumor progression. *Nat Protoc* **2**, 1998–2004.

[7] Baba M, Furihata M, Hong SB, Tessarollo L, Haines DC, Southon E, Patel V, Igarashi P, Alvord WG, Leighty R, et al. (2008). Kidney-targeted Birt-Hogg-Dube gene inactivation in a mouse model: Erk1/2 and Akt-mTOR activation, cell hyperproliferation, and polycystic kidneys. *J Natl Cancer Inst* **100**, 140–154.

[8] Kinner S and Lauenstein TC (2007). MR colonography. *Radiol Clin North Am* **45**, 377–387.

[9] Lauenstein TC, Herborn CU, Vogt FM, Gohde SC, Debatin JF, and Ruehm SG (2001). Dark lumen MR-colonography: initial experience. *Rofo* **173**, 785–789.

[10] Rasband WS (1997–2007). *Image J* Bethesda, MD: US National Institutes of Health.

[11] Okayasu I, Hatakeyama S, Yamada M, Ohkusa T, Inagaki Y, and Nakaya R (1990). A novel method in the induction of reliable experimental acute and chronic ulcerative colitis in mice. *Gastroenterology* **98**, 694–702.

[12] Ajaj W, Pelster G, Treichel U, Vogt FM, Debatin JF, Ruehm SG, and Lauenstein TC (2003). Dark lumen magnetic resonance colonography: comparison with conventional colonoscopy for the detection of colorectal pathology. *Gut* **52**, 1738–1743.

[13] Beets-Tan RG and Beets GL (2004). Rectal cancer: review with emphasis on MR imaging. *Radiology* **232**, 335–346.

[14] Johnson CD, Chen MH, Toledano AY, Heiken JP, Dachman A, Kuo MD, Menias CO, Siewert B, Cheema JI, Obregon RG, et al. (2008). Accuracy of

CT colonography for detection of large adenomas and cancers. *N Engl J Med* **359**, 1207–1217.

[15] Saar B, Gschossmann JM, Bonel HM, Kickuth R, Vock P, and Netzer P (2008). Evaluation of magnetic resonance colonography at 3.0 tesla regarding diagnostic accuracy and image quality. *Invest Radiol* **43**, 580–586.

[16] Hartmann D, Bassler B, Schilling D, Adamek HE, Jakobs R, Pfeifer B, Eickhoff A, Zindel C, Riemann JF, and Layer G (2006). Colorectal polyps: detection with dark-lumen MR colonography *versus* conventional colonoscopy. *Radiology* **238**, 143–149.

[17] Lam WW, Leung WK, Wu JK, So NM, and Sung JJ (2004). Screening of colonic tumors by air-inflated magnetic resonance (MR) colonography. *J Magn Reson Imaging* **19**, 447–452.

[18] Lomas DJ, Sood RR, Graves MJ, Miller R, Hall NR, and Dixon AK (2001). Colon carcinoma: MR imaging with CO_2 enema—pilot study. *Radiology* **219**, 558–562.

[19] Hensley HH, Chang WC, and Clapper ML (2004). Detection and volume determination of colonic tumors in Min mice by magnetic resonance microimaging. *Magn Reson Med* **52**, 524–529.

[20] Kacmarek RM, Wiedemann HP, Lavin PT, Wedel MK, Tutuncu AS, and Slutsky AS (2006). Partial liquid ventilation in adult patients with acute respiratory distress syndrome. *Am J Respir Crit Care Med* **173**, 882–889.

[21] Leach CL, Greenspan JS, Rubenstein SD, Shaffer TH, Wolfson MR, Jackson JC, DeLemos R, and Fuhrman BP (1996). Partial liquid ventilation with perflubron in premature infants with severe respiratory distress syndrome. The LiquiVent Study Group. *N Engl J Med* **335**, 761–767.

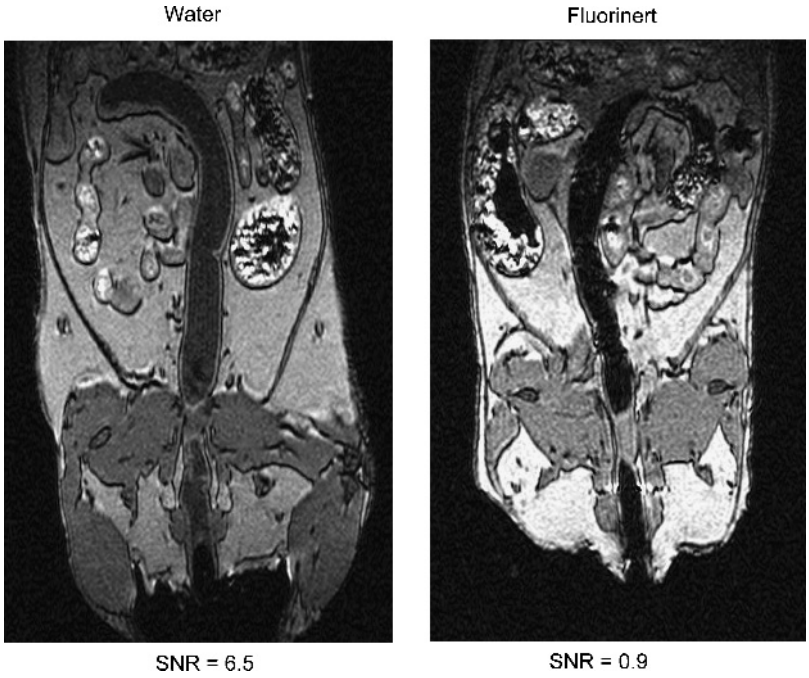

Figure W1. T1W images of mouse colon after water or Fluorinert enema.